

Received: 2018.01.07  
Accepted: 2018.05.05  
Published: 2018.08.10

# Comparison of Contrast-Enhanced Ultrasound and Positron Emission Tomography/Computed Tomography (PET/CT) in Lymphoma

Authors' Contribution:  
Study Design A  
Data Collection B  
Statistical Analysis C  
Data Interpretation D  
Manuscript Preparation E  
Literature Search F  
Funds Collection G

EF 1 **Xiaoyan Niu\***  
EF 1 **Wenbin Jiang\***  
B 1 **Xiaojuan Zhang**  
B 1 **Zhaoyan Ding**  
D 2 **Hongwei Xue**  
C 3 **Zhenguang Wang**  
A 1 **Cheng Zhao**

1 Department of Ultrasound, The Affiliated Hospital of Qingdao University, Qingdao, Shandong, P.R. China  
2 Department of Lymphoma, The Affiliated Hospital of Qingdao University, Qingdao, Shandong, P.R. China  
3 Department of Nuclear Medicine, The Affiliated Hospital of Qingdao University, Qingdao, Shandong, P.R. China

\* These authors contributed equally to this work and should be considered co-first authors

**Corresponding Author:** Cheng Zhao, e-mail: [zhaochengdr@163.com](mailto:zhaochengdr@163.com)

**Source of support:** Our study was funded by the Medical Science and Technology Development Project of Shandong Province (No. 2016WS0284)

**Background:** This study aimed to assess the value of contrast-enhanced ultrasound (CEUS) in the diagnosis and prognosis of lymphoma based on PET-CT.





**Material/Methods:** Our study included 88 superficial lymph nodes and 63 patients who underwent ultrasound-guided biopsy or surgery for pathology from October 2015 to March 2017. All lymph nodes were assessed by CEUS and PET-CT. CEUS and PET-CT parameters were recorded, including arrive time (AT), time to peak (TTP), base intensity (BI), peak intensity (PI), ascending slope (AS), descending slope (DS), area under the TIC curve (AUC), maximum standardized uptake value (SUVmax), and mean standardized uptake value (SUVmean). Pearson's correlation was used to assess the associations of CEUS and PET-CT parameters.

**Results:** Of the 88 lymph nodes examined, 12 were Hodgkin's lymphoma (HL) and 76 were non-Hodgkin's lymphoma (NHL). The variations of CEUS dose parameters ( $\Delta I$ , AUC, and AS) were positively correlated with PET-CT results (SUVmax and TLG). Correlation coefficients were 0.609, 0.518, 0.456, 0.630, 0.593, and 0.532, respectively. The remaining time values (AT, TP, and  $\Delta T$ ) were negatively associated with PET-CT results. Correlation coefficients were -0.239, -0.272, -0.284 and -0.377, -0.391, and -0.320, respectively.

**Conclusions:** Quantitative CEUS data were correlated with PET-CT values, with potential use in the diagnosis of lymphoma.

**MeSH Keywords:** **Evaluation Studies as Topic • Lymph Nodes • Positron-Emission Tomography • Ultrasonography**

**Full-text PDF:** <https://www.medscimonit.com/abstract/index/idArt/908849>

 2892  4  3  26



## Background

Lymphoma is a group of highly heterogeneous diseases, with a number of pathological types, especially for non-Hodgkin's lymphoma (NHL). The incidence of lymphoma is increasing around the world. Studies have proposed that its incidence in developed countries is higher than in developing countries [1]. However, with economic development, increasingly prominent environmental pollution, and population accretion and aging, lymphoma incidence in developing countries is increasing. Lymphoma detection and staging rely on PET-CT by combining structural and functional imaging. However, there are some drawbacks; e.g., the results can only reflect the metabolism of lesions in fixed time and the examination cannot be repeated in a short time because of high cost and adverse effects of radiation. Although increasing PET-CT values indicate that tumor cells grow rapidly and metabolize vigorously, these high values cannot differentiate malignant tumors. Meanwhile, malignant lesions and hyperplastic lymph nodes cannot be differentiated in evaluating the therapeutic effects [2,3].

Ultrasound is considered the first choice for detecting superficial lymph nodes. CEUS, an advanced ultrasound technique, is superior to color Doppler in the detection of microvessels and can obviously improve the diagnostic value of traditional and color Doppler ultrasound [4]. However, use of CEUS in the diagnosis and treatment of lymphoma is rather rare. By use of real-time dynamic imaging, enhanced intensity, extent, and pattern of the lymph node can be clearly observed and the time-intensity curve (TIC) can be drawn and analyzed. Therefore, with qualitative and quantitative data, a more comprehensive and objective understanding of the internal structure's characteristics and activated state of lymph nodes can be provided. In this study, we compared CEUS and PET-CT results to evaluate the utility of CEUS in lymphoma.

## Material and Methods

From October 2015 to March 2017, 63 patients with a total of 88 superficial lymph nodes were enrolled in our hospital. All lymph nodes underwent CEUS and PET-CT, with ultrasound-guided biopsy or surgery for pathology. Some patients were excluded due for contraindications of contrast agent (under 18 years old or pregnancy) and PET-CT (glucose poorly controlled). This study was approved by the Ethics Committee of our hospital and informed consent was obtained from all patients participating in the study.

### CEUS imaging strategy in lymphoma patients

All patients were examined in the cervical, axillary, and inguinal regions by traditional and color Doppler ultrasound techniques.

Suspicious lymph nodes underwent CEUS by 2 ultrasound physicians with at least 5 years of experience and who unaware of the patients' histopathology. All ultrasound examinations were obtained on a scanner (GE Logic E8, CT) and a 9L high-frequency linear array transducer before the first cycle of chemotherapy. The characteristics of the nodes of interest were recorded, including diameter, peak velocity, and elastic strain rate. Then, the largest section was selected for CEUS. Contrast/General preset and a low mechanical index (0.11) were used, recording for approximately 90 s. The second-generation sulfur hexafluoride microbubble contrast SonoVue (Bracco SpA, Milan, Italy), approved for diagnostic imaging in China, was used in the evaluations. All patients provided informed consent for intravenous use of the contrast agent. A 2.4-mL dose of the contrast agent was bolus-injected into a peripheral vein, followed by the injection of 5 ml of physiological saline solution. The lymph nodes were scanned immediately, keeping continuous records and saving the images.

Enhancement intensity was divided into intense, moderate, and weak enhancement (degree of lymph node enhancement higher, equal to, or lower than the surrounding normal tissue, respectively). The extent of node enhancement was homogeneous (global or diffuse enhancement) or heterogeneous (partial filling defect in the lymph nodes). Enhancement pattern was central (microbubble from the edge of the lymph node to the center) or centrifugal (global and diffuse enhancement, or from the hilum of lymph node to the surrounding area). The boundary of enhanced lymph nodes can be divided into clear (circumference of the node more than 50% with a well-defined border) and unclear (blurred border, lobulated and angulate appearance, or circumference of the node less than 50% with a well-defined border).

The fast and remarkable perfusion area of a lymph node was selected as the region of interest (ROI) [5]. The sample frame was circular, with size associated with the node diameter. For each patient, ROI in lesions were assessed 3 times, and the mean ROI value was considered the final value. The results of lymphoma CEUS were analyzed as time-intensity curve (TIC) by the built-in software. Then, the following time and dose parameters were recorded: arrive time (AT) (in seconds), defined as the first point of the curve clearly above the baseline intensity; time to peak (TTP) (in seconds), defined as the time to maximum curve intensity;  $\Delta T = TTP - AT$ ; base intensity (BI) (in dB), defined as the intensity at arrival time; peak intensity (PI) (in dB), defined as the intensity at peak time;  $\Delta I = PI - BI$ ; area under the curve (AUC), calculated integral for the time-intensity curve; ascending slope (AS), defined as the maximum wash-in velocity of the contrast medium; and descending slope (DS), defined as the maximum wash-out velocity of the contrast medium. The change of velocity and flow with time after injection of contrast agent was reflected by the above

parameters. Time and intensity values were calculated from the fitted curve and not raw-image data.

### PET-CT imaging strategy in lymphoma patients

<sup>18</sup>F-FDG PET-CT scanning was performed in the same week as CEUS before the first cycle of chemotherapy in all enrolled patients. Each patient fasted for 4–6 h before scanning, which was verified by blood glucose levels of 4.5–8.2 ml/l. They were administered intravenous injections of 0.015–0.18 mCi/kg <sup>18</sup>F-FDG and placed in the supine position for 60 min to avoid muscular uptake. Then, PET-CT scanning was performed on a Discovery ST PET-CT scanner (GE Healthcare, CT, USA) from skull base to the upper thigh after micturition. CT and PET imaging data were transmitted to a Workstation device (Xeleris, GE Healthcare, CT, USA), which was used for image display and analysis. PET-CT images were read by 2 radiologists unaware of any clinical or radiological information. The same lymph nodes and ROIs were chosen to calculate the maximum standardized uptake value (SUV<sub>max</sub>) and total lesion glycolysis (TLG), with  $TLG = SUV_{mean} * MTV$  (mean standardized uptake value, SUV<sub>mean</sub>; metabolic tumor volume, MTV) [6]. We first automatically sketched an interesting area, which was over 30% of the threshold uptake values by visual analysis, followed by manual sketch of the original site's boundary, combined with the morphological performance from CT imaging. Finally, the volume of each layer was obtained by the area of each layer multiplied by its thickness, and MTV was derived by use of an accumulation algorithm.

### Design ideas

Firstly, correlations between CEUS and PET-CT values were analyzed in all enrolled lymph nodes. Then, lymph nodes were divided into early-stage, advanced stage, HL, NHL, B cell lymphoma, T cell lymphoma, aggressive lymphoma, and indolent lymphoma; clinical staging defined I and II as early-stage, and III and IV as advanced stage, and pathological types referred to the World Health Organization classification of tumors of hematopoietic and lymphoid tissues in 2008 [7]. The associations of CEUS parameters for different staging and pathological types with corresponding PET-CT values were explored in different groups.

### Statistical analysis

Statistical analyses were performed with SPSS version 19.0 for Windows (SPSS Inc., Chicago, IL). Data are expressed as mean  $\pm$ SD, and comparisons between CEUS and PET-CT parameters were assessed by Pearson correlation.  $P < 0.05$  was considered statistically significant. Correlation coefficient values  $< 0.30$  indicated a weak correlation, 0.31–0.80 indicated a moderate correlation, and  $> 0.80$  indicated a high correlation.

### L1 Results

There were 42 male and 21 female patients, aged from 20 to 74 (median, 50) years. Sixty-four cases had lymph nodes in the neck, 10 in the axillary region and 14 in the inguinal region. Staging distribution revealed 17 early-stage lymphomas and 71 advanced lymphomas. Histopathological results revealed 12 Hodgkin's lymphoma (HL) and 76 non-Hodgkin's lymphoma (NHL), including 40 diffuse large B cell lymphomas (DLBCL), 14 follicular lymphomas (FL), 6 extranodal NK/T cell lymphomas (ENK/TCL), 6 anaplastic large B cell lymphomas (ALBCL), 4 mantle cell lymphomas (MCL), 4 T-lymphoblastic lymphomas (TLL), and 2 precursor T cell lymphomas (PTCL). Node diameters in the longitudinal axis were  $2.95 \pm 1.20$  cm (range 0.7–5.0 cm), the elasticity (E) imaging stiffness ratio of nodes averaged  $3.95 \pm 0.77$  (range 2.3–5.5), and color Doppler flow resistance index (RI) of the nodes averaged  $0.60 \pm 0.09$  (range 0.42–0.75). CEUS and PET-CT data are summarized in Table 1.

### Qualitative results of contrast-enhanced ultrasound

Qualitative specific results of CEUS are summarized in Table 2. A total of 67/88 (76.1%) nodes had intense enhancement, 17 of 88 (19.3%) had moderate enhancement, and 4 showed weak enhancement. Homogeneous enhancement was documented in 77 of 88 nodes (87.5%) and heterogeneous enhancement in 11 nodes (12.5%). The enhancement pattern of 74 nodes (85.2%) was centrifugal, including 47 with global and diffuse enhancement and 27 with micro-bubbles from the lymph node's hilum to the surrounding area; 14 nodes (15.7%) showed central enhancement. The boundary of 80 (90.9%) enhanced lymph nodes was clear and 8 (9.1%) nodes had unclear boundaries.

### Correlation between CEUS and PET-CT parameters

TIC parameters for each ROI were compared with SUV<sub>max</sub> and TLG. Moderate positive correlations were observed between  $\Delta I$  ( $r = 0.609$ ,  $p = 0.000$ ,  $r = 0.630$ ,  $p = 0.000$ ), AUC ( $r = 0.518$ ,  $p = 0.000$ ,  $r = 0.593$ ,  $p = 0.000$ ), and AS ( $r = 0.456$ ,  $p = 0.000$ ,  $r = 0.532$ ,  $p = 0.000$ ) and SUV<sub>max</sub> and TLG. AT, TTP, and  $\Delta T$  were low-moderately negatively related to SUV<sub>max</sub> ( $r = -0.239$ ,  $P = 0.025$ ,  $r = -0.272$ ,  $P = 0.010$ ,  $r = -0.284$ ,  $P = 0.007$ ) and TLG ( $r = -0.377$ ,  $P = 0.000$ ,  $r = -0.391$ ,  $P = 0.000$ ,  $r = -0.320$ ,  $p = 0.002$ ). For the different pathological types and clinical stages, the general and specific correlations between CEUS and PET-CT are summarized in Tables 3 and 4. The manifestations of enlarged lymph nodes in the same patient are shown in Figures 1–3.

### Discussion

CEUS is a new microvessel detecting technology, which can detect diameters less than 40  $\mu$ m and identify vascular changes

**Table 1.** Characteristics of the contrast-enhanced US enhancement parameters and PET/CT SUVmax.

Characteristic	Range	Mean ± standard deviation	Characteristic	Range	Mean ± standard deviation
AT (arrive time)	6.0~19.0	13.39±3.06	DS (descending slope)	0.2~2.4	0.69±0.49
TTP (time to peak)	10.0~25.0	19.05±3.49	Area under curve of TIC	144.10~1063.81	478.37±210.08
ΔT	3.0~8.0	5.68±1.13	SUVmax	2.1~25.2	7.44±6.15
BI (base time)	-70~-43	-56.17±5.56	SUVmean	0.6~17.0	4.72±4.10
PI (peak intensity)	-55~-28	-40.57±5.28	MTV	0.25~59.52	12.30±14.91
ΔI	10~21	15.63±1.96	TLG	0.4~510.87	74.67±115.58
AS (ascending slope)	1.43~5.25	2.89±0.84			

**Table 2.** Qualitative results of CEUS.

Pathological type	CEUS									
	Enhanced intensity			Enhanced degree		Enhanced pattern		Boundary		
	Intense	Moderate	Weak	Homogeneous	Heterogeneous	Central	Centrifugal	Clear	Unclear	
HL	10	2	0	12	0	2	10	12	0	
DLBL	28	12	0	32	8	10	30	34	6	
FL	12	0	2	13	1	0	14	13	0	
NK/TCL	4	2	0	6	0	0	6	6	0	
ML	3	1	0	4	0	0	4	4	0	
ALBCL	6	0	0	4	2	2	4	4	2	
TLL	3	0	1	4	0	0	4	4	0	
PTL	1	0	1	2	0	0	2	2	0	

**Table 3.** Relationship between contrast-enhanced US parameters and PET/CT values in all patients with lymphoma.

CEUS parameters	SUVmax		TLG	
	P Values	Pearson's correlation coefficients	P values	Pearson's correlation coefficients
AT	0.025	-0.239	0.000	-0.377
TTP	0.010	-0.272	0.000	-0.391
ΔT	0.007	-0.284	0.002	-0.320
BI	0.259	-0.122	0.056	-0.205
PI	0.359	0.099	0.861	0.019
ΔI	0.000	0.609	0.000	0.630
AS	0.456	0.000	0.000	0.532
DS	0.563	-0.062	0.893	-0.015
AUC of TIC	0.000	0.518	0.000	0.593

**Table 4.** Relationship between contrast-enhanced US parameters and PET/CT values in patients with different types of lymphoma.

Type of lymphoma	CEUS parameters								
	AT (r,P)	TP (r,P)	ΔT (r,P)	BI (r,P)	TI (r,P)	ΔI (r,P)	AUC (r,P)	AS (r,P)	DS (r,P)
Early (compare with SUVmax)	-0.343	-0.431	-0.270	-0.062	0.092	0.566	0.491	0.456	-0.151
	0.178	0.084	0.294	0.814	0.726	0.018	0.045	0.066	0.564
Early (compare with TLG)	-0.422	-0.517	-0.289	-0.316	0.116	0.768	0.609	0.497	0.040
	0.092	0.034	0.261	0.216	0.657	0.000	0.009	0.042	0.879
Advanced (compare with SUVmax)	-0.247	-0.294	-0.342	-0.140	0.099	0.631	0.534	0.510	-0.070
	0.037	0.013	0.003	0.244	0.409	0.000	0.000	0.000	0.563
Advanced (compare with TLG)	-0.376	-0.386	-0.327	-0.186	0.042	0.609	0.591	0.531	-0.039
	0.001	0.001	0.005	0.119	0.729	0.000	0.000	0.000	0.745
HL (compare with SUVmax)	-0.495	-0.610	-0.686	0.089	0.527	0.746	0.740	0.827	-0.381
	0.102	0.035	0.014	0.783	0.079	0.005	0.006	0.001	0.222
HL (compare with TLG)	-0.392	-0.527	-0.670	-0.136	0.264	0.660	0.801	0.764	-0.195
	0.207	0.078	0.017	0.674	0.407	0.020	0.002	0.004	0.543
NHL (compare with SUVmax)	-0.379	-0.346	-0.250	-0.145	0.058	0.650	0.593	0.435	-0.065
	0.001	0.002	0.030	0.211	0.618	0.000	0.000	0.000	0.577
NHL (compare with TLG)	-0.388	-0.366	-0.294	-0.203	0.000	0.662	0.560	0.518	-0.007
	0.001	0.001	0.010	0.079	0.998	0.000	0.000	0.000	0.955
Aggressive (compare with SUVmax)	-0.387	-0.338	-0.274	-0.163	0.053	0.657	0.668	0.467	-0.086
	0.002	0.007	0.031	0.207	0.681	0.000	0.000	0.000	0.764
Aggressive (compare with TLG)	-0.403	-0.378	-0.365	-0.222	-0.010	0.663	0.611	0.567	-0.017
	0.001	0.002	0.004	0.083	0.939	0.000	0.000	0.000	0.893
Indolent (compare with SUVmax)	-0.196	0.090	0.449	-0.415	-0.412	-0.505	0.191	-0.407	-0.382
	0.502	0.759	0.107	0.140	0.143	0.066	0.513	0.149	0.177
Indolent (compare with TLG)	-0.039	0.180	0.403	-0.245	-0.113	0.040	-0.005	-0.209	-0.088
	0.894	0.538	0.154	0.399	0.700	0.893	0.985	0.473	0.764
B cell (compare with SUVmax)	-0.362	-0.322	0.218	-0.183	0.019	0.614	0.582	0.385	0.010
	0.003	0.010	0.084	0.147	0.881	0.000	0.000	0.002	0.937
B cell (compare with TLG)	-0.373	-0.353	-0.293	-0.197	0.020	0.660	0.559	0.506	0.013
	0.002	0.004	0.019	0.118	0.874	0.000	0.000	0.000	0.920
T cell (compare with SUVmax)	-0.732	-0.784	-0.730	0.104	0.286	0.877	0.784	0.864	-0.214
	0.007	0.003	0.007	0.747	0.367	0.000	0.004	0.000	0.505
T cell (compare with TLG)	-0.806	-0.780	-0.582	-0.287	-0.121	0.769	0.680	0.698	0.011
	0.002	0.003	0.047	0.366	0.707	0.003	0.021	0.012	0.973

in the tumor. This technology has many advantages, including low cost, safety, and repeatability in a short time, and can provide more information on perfusion for evaluating the physiopathological characteristic of lymph nodes by real-time dynamic imaging of microcirculation blood flow perfusion [8,9]. Its use in blood vessels, the liver, and the kidneys has reached wide consensus and is generally recognized [10,11]. However, in lymphadenopathy, CEUS is rarely used, and no universal standard has been agreed on. Currently, CEUS is more popular in lymph node evaluation, and studies showed that its use can improve the ultrasound diagnostic level, with sensitivity and specificity of 84~98% and 54.5~92%, respectively, and a diagnostic accuracy of 76.3~92.8% [12-16].

There has been no published report comparing CEUS and PET-CT in qualitative analysis, because CEUS is a real-time dynamic imaging process and PET-CT is a fixed-time scanning method. Dynamic imaging can provide much more information for lymph node evaluation. Most lymph nodes show hilar vascularity. The explanation offered for such a pattern is that malignant cells originate in lymph nodes and grow in a centrifugal pattern [17]. Xianshui et al. [18] reported that the blood supply pattern in lymphoma is correlated to the level of malignancy. In low-grade lymphoma the blood flow is eccentric or altered with or without radial branching in lymph nodes, while in high-grade lymphoma the blood flow is subcapsular, hybrid-meshed, or multicenter hilar. These blood flow

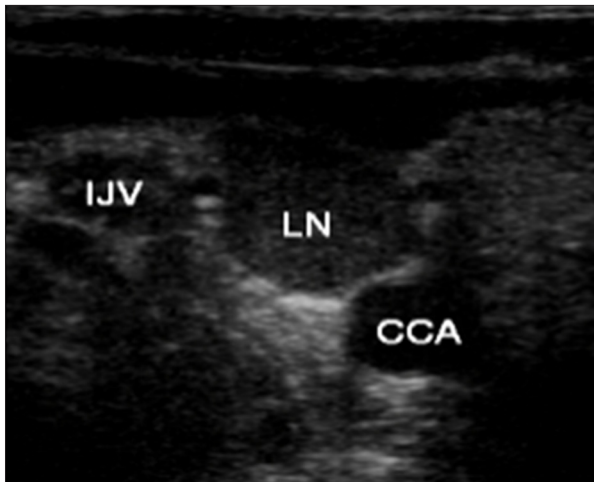


**Figure 1.** Two-dimensional ultrasound image. A large lymph node is seen between the carotid artery and the internal jugular vein. CCA – common carotid artery; IJV – internal jugular vein; LN – lymph node

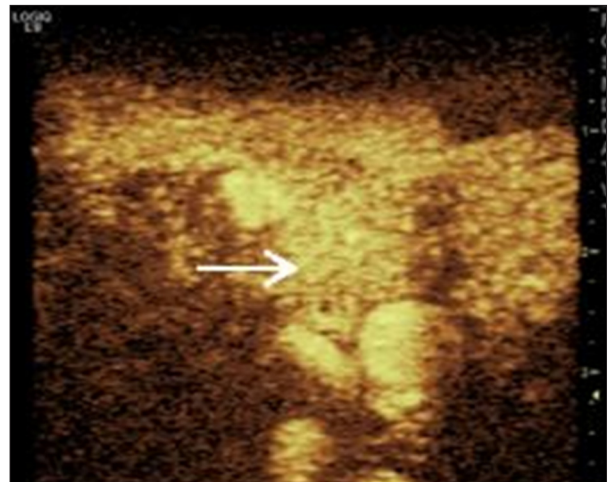


**Figure 2.** Contrast enhancement image. The enhanced pattern of the enlarged lymph node (arrow indicates the enhanced lymph node) is homogeneous and intense. TTP=17 s,  $\Delta I=18$ .

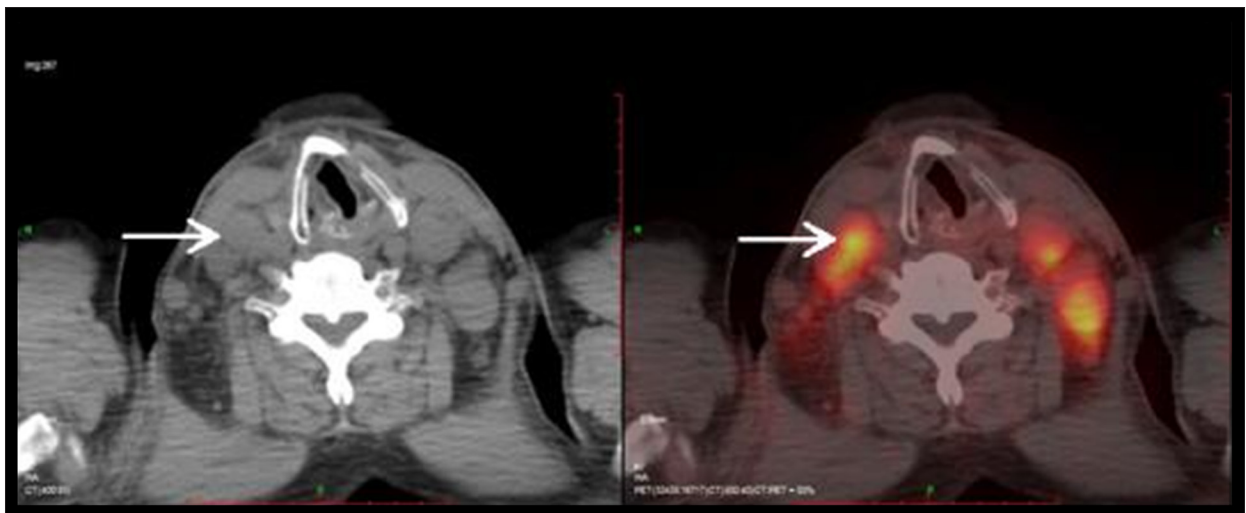


**Figure 3.** PET/CT image of the same patient. The corresponding enlarged lymph node (the arrow indicates the lymph node with enhanced metabolism) shows increased metabolism and SUVmax=11.2.

characteristics can be detected easily and sensitively by CEUS. The 88 lymph nodes assessed here showed central enhancement (14 nodes) or centrifugal enhancement (74 nodes, including 47 global/diffuse and 27 hilar enhancement, respectively). The global and diffuse enhancement patterns found in the present study are typical of lymphoma, as reported by Rubaltelli et al. [12] in the following terms: diffuse enhancement of snowy dotted pattern in the beginning, with these bright spots merging to form homogeneous enhancement. This phenomenon is caused by the high hyperplasia of blood vessels. Micro-bubbles can perfuse and spread rapidly in the whole lymph node, rarely with filling defect; this results in naturally enlarged vessels from the hilum to the periphery, which is typical for the enhancement pattern [19]. Radka Slaisova et

al. [16] reported that intense homogeneous enhancement can be visualized in 53 of 60 (88.3%) nodes. The present study visualized intense enhancement in 67 of 88 (79.8%), and homogeneous enhancement in 77 of 88 (87.5%). According to Yu et al. [14], the typical enhancement pattern for T cell lymphoma is homogeneous but is filling defect for B cell type. In the present study, all 11 heterogeneous enhancement nodes were B cell lymphoma (8 DLBCL, 2 ALBCL, and 1 FL). However, B cell lymphoma still mainly showed homogeneous enhancement 76.6% (49/64). Although showing different intensities, NHL of T cell source and HL all showed homogeneous enhancement in the present study.

CEUS' TIC can assess spatial and temporal variations in the tumor microcirculation. Some parameters ( $\Delta I$  and AUC) are more correlated with the local blood volume of the indicated region (mL) while others reflect more blood flow (TTP and  $\Delta T$ ) parameters. The potential application of CEUS in lymphoma can be intuitively reflected by the conclusion from associations of these parameters and PET-CT values. Previous data suggest strong associations of intratumoral microvessel density (MVD) and CEUS parameters [20–22]. In the current lymph nodes,  $\Delta I$ , AUC, and AS showed positive associations with PET-CT values. Therefore, the richer the capillaries, the faster the filling velocity and the greater the filling dose after contrast agent injection into the blood vessels. Meanwhile, the growth and development of new microvessels is required for solid tumors to expand in size. Therefore, the richer the new blood vessels in lymph nodes, the more vigorous the tumor cell metabolism; PET-CT values increase accordingly. Time parameters such as AT, TTP, and  $\Delta T$  were negatively correlated with PET-CT values, suggesting that the more vessels in lymph nodes, the more vigorous the tumor cell metabolism; arrival time and time to peak of contrast agent increase accordingly. The associations of the parameters were generally moderate. Dose parameters of CEUS were moderately related to PET/CT values, while most time parameters had a weak relationship. It may be that the PET/CT value SUVmax and TLG are the dose parameters, so it is more directly comparable to the  $\Delta I$  and AUC parameters of the dose-value, while the time parameters can only indirectly reflect the uptake of the lesion to the  $^{18}F$ -FDG.

In the analysis of different pathological types and clinical stages, in HL, the present report demonstrated a significant correlation between AS and SUVmax ( $r=0.827$ ) and a high correlation between AUC and TLG ( $r=0.801$ ). A possible explanation is that the HL type is relatively homogenous, while the NHL pathological type is heterogeneous, and the same type may be in a phase of different tumor proliferations. Several previous studies have shown the clear diagnostic value of PET-CT in HL and high-grade NHL; however, its use in low-grade NHL remains controversial [23–25]. HL and aggressive NHL showed a correlation between CEUS and PET-CT, but indolent NHL showed no such correlation. One explanation may be that although indolent lymphoma is well differentiated, it has a normal lymph node blood flow and the metabolic level is low. Regarding the source of T cell lymphoma, there was a strongly positive correlation between  $\Delta I$ , AS, and SUVmax ( $r=0.877$ ,  $0.864$ ) and a strongly negative correlation between AT and TLG ( $r=-0.806$ ),

probably due to the small number of pathological types of T cell lymphoma and the highly invasive types of our study. Thus, the biological behavior is more consistent. In the present study there were no associations of CEUS with PET-CT parameters in some pathological types and clinical stages of lymphoma such as the time parameters in early lymphoma and HL, which may be related to the reduced number of cases; e.g., early lymphoma in 17 cases and 12 HL cases. There was no significant correlation between BI and PI and PET/CT parameters in this study, which may be due to differences between individuals in metabolism of contrast agents.

This study had some limitations. Firstly, the sample size was relatively small, especially for lymphoma, which contains various pathological types, and the association of CEUS with PET-CT remains unclear. Secondly, the limited scanning areas during sonography make it impossible for CEUS to detect all lesions simultaneously, which limits use of CEUS in predicting lymphoma in the whole body. In addition, for some special sites such as mediastinal and retro peritoneal lymph node enlargement, the effect of superficial ultrasound is limited.

## Conclusions

The utility of PET-CT in the diagnosis and staging of lymphoma is widely recognized [26]. However, this method has inevitable disadvantages, and performing PET-CT with the detection of new suspicious superficial lymph nodes is not the best option. CEUS, as a cost-effective and safe method, is becoming the optimal method for assessing suspicious nodes. Indeed, CEUS provides a detailed initial evaluation of lymph nodes by repeated non-invasive examinations during clinical diagnosis. The real-time enhancement process and TIC parameters can provide comprehensive information regarding the activity of lymph nodes for further examination. CEUS is limited in evaluating lymphoma only by the enhancement pattern. Conventional ultrasound, color Doppler ultrasound, and CEUS are supposed to assess the nodes in combination. Lymphoma is generally characterized by multiple enlarged lymph nodes; CEUS examination was performed for the most significance lymph node, with dynamic enhancement and TIC analyzed to provide reliable evidence for defining the tumor properties. In addition, CEUS, with the advantage of capillary detection in the lymphoma, is of potential research value in assessing the chemotherapeutic effects.

## References:

1. Torre L A, Bray F, Siegel RL et al: Global cancer statistics, 2012. *Cancer J Clin*, 2015, 65(2): 87–108
2. Avivi I, Zilberlicht A, Dann EJ et al: Strikingly high false positivity of surveillance FDG PET-CT scanning among patients with diffuse large cell lymphoma in the rituximab era. *Am J Hematol*, 2013; 88: 400–5
3. Querellou S, Valette F, Bodet-Milin C et al: FDG PET-CT predicts outcome in patients with aggressive non-Hodgkin's lymphoma and Hodgkin's disease. *Ann Hematol*, 2006; 85: 759–67
4. Weskott HP: Emerging roles for contrast-enhanced ultrasound. *Clin Hemorheol Microcirc*, 2008; 40(1): 51–71
5. Zhang HP, Shi QS, Li F et al: Regions of interest and parameters for the quantitative analysis of contrast-enhanced ultrasound to evaluate the anti-angiogenic effects of bevacizumab. *Mol Med Rep*, 2013; 8(1): 154–60
6. Thomas C, Franck M, Maximilien V et al: Pre-therapy 18F-FDG PET quantitative parameters help in predicting the response to radioimmunotherapy in non-Hodgkin lymphoma. *Eur J Nucl Med Mol Imaging*, 2010; 37(3): 494–504
7. Swerdlow SH, Campo E, Hans N Let al. (eds.), World Health Organization classification of tumor of haematopoietic and lymphoid tissues. Lyon: IARC, 2008
8. Lassau N, Lamuraglia M, Chami L et al: Gastrointestinal stromal tumors treated with imatinib: monitoring response with contrast-enhanced sonography. *Am J Roentgenol*, 2006; 187(5): 1267–73
9. Lassau N, Chebil M, Chami L et al: Dynamic contrast-enhanced ultrasonography (DCE-US): A new tool for the early evaluation of antiangiogenic treatment. *Target Oncol*, 2010; 5(1): 53–58
10. Liu GJ, Lu MD, Xie XY et al: Real-time contrast-enhanced ultrasound imaging of infected focal liver lesions. *J Ultrasound Med*, 2008; 27: 657–66
11. Albrecht T, Thorelius L, Solbiati L et al. (eds.), Contrast-enhanced ultrasound in clinical practice-liver, prostate, pancreas, kidney and lymph nodes. Milan: Springer, 2005: 38–50
12. Rubaltelli L, Khadivi Y, Tregnaghi A et al: Evaluation of lymph node perfusion using continuous mode harmonic ultrasonography with a second-generation contrast agent. *J Ultrasound Med*, 2004; 23: 829–36
13. Rubaltelli L, Corradin S, Dorigo A et al: Automated quantitative evaluation of lymph node perfusion on contrast-enhanced sonography. *Am J Roentgenol*, 2007; 188(4): 977–83
14. Yu M, Liu Q, Song HP et al: Clinical application of contrast-enhanced ultrasonography in diagnosis of superficial lymphadenopathy. *J Ultrasound Med*, 2010; 29: 735–40
15. Pei XQ, Liu LZ, Zheng W et al: Contrast-enhanced ultrasonography of hepatocellular carcinoma: Correlation between quantitative parameters and arteries in neoangiogenesis or sinusoidal capillarization. *Eur J Radiol*, 2012; 81(3): e182–88
16. Slaisova R, Benda K, Jarkovsky J et al: Contrast-enhanced ultrasonography compared to gray-scale and power Doppler in the diagnosis of peripheral lymphadenopathy. *Eur J Radiology*, 2013; 82(4): 693–98
17. Giovagnorio F, Galluzzo M, Andreoli C et al: Color Doppler sonography in the evaluation of superficial lymphomatous lymph nodes. *J Ultrasound Med*, 2002; 21: 403–8
18. Fu XS, Tang J, Su L et al: Differential diagnosis of superficial lymphadenopathy with color Doppler flow imaging. *Chin J Ultrasonogr*, 2003; 12(7): 420–22
19. Stramare R, Scagliori E, Mannucci M et al: The role of contrast-enhanced gray-scale ultrasonography in the differential diagnosis of superficial lymph nodes. *Ultrasound Q*, 2010, 26(1): 45–51
20. Zheng W, Xiong Y, Han J et al: Contrast-enhanced ultrasonography of cervical carcinoma: Perfusion pattern and relationship with tumour angiogenesis. *Br J Radiol*, 2016; 89(1065): 20150887
21. McCarville MB, Streck CJ, Dickson PV et al: Angiogenesis inhibitors in a murine neuroblastoma Model: Quantitative assessment of intratumoral blood flow with contrast-enhanced gray-scale US. *Radiology*, 2006; 240: 73–81
22. Wang Z, Tang J, An L et al: Contrast-enhanced ultrasonography for assessment of tumor vascularity in hepatocellular carcinoma. *J Ultrasound Med*, 2007; 26: 757–62
23. Elstrom R, Guan L, Baker G et al: Utility of FDG PET scanning in lymphoma by WHO classification. *Blood*, 2003; 101(10): 3875–76
24. Jerusalem G, Beguin Y, Najjar F et al: Positron emission tomography (PET) with 18F-fluorodeoxyglucose (18F-FDG) for the staging of low-grade non-Hodgkin's lymphoma (NHL). *Ann Oncol*, 2001; 12: 825–30
25. Karam M, Novak L, Cyriac J et al: Role of fluorine-18 fluoro-deoxy glucose positron emission tomography scan in the evaluation and follow-up of patients with low-grade lymphomas. *Cancer*, 2006; 107(1): 175–83
26. Fallanca F, Alongi P, Incerti E et al: Diagnostic accuracy of FDG PET-CT for clinical evaluation at the end of treatment of HL and NHL: A comparison of the Deauville Criteria (DC) and the International Harmonization Project Criteria (IHPC). *Eur J Nucl Med Mol Imaging*, 2016; 43(10): 1837–48